Z_2 oscillations and target-structure effects in the electronic stopping cross section of heavy ions in solids

I. Gertner, M. Meron, and B. Rosner
Department of Physics, Technion—Israel Institute of Technology, Haifa, Israel
(Received 24 May 1979)

The density model that was successfully used to obtain electronic stopping cross sections for slow-moving heavy ions traversing solid media was applied to estimate the well-known Z_2 oscillations in these cross sections. Good agreement with experimental results was generally found. Some of the possible sources of discrepancy are discussed. Relations between the results of Compton-profile measurements which depend on the bulk properties of the solid and the electronic stopping in thin foil targets assist in resolving ambiguities in the Z_2 dependence of the experimental results. It is concluded that the electronic stopping cross sections are not a universal function of E, Z_1, and Z_2. They depend strongly on the method of the preparation of the target foil and on its history.

I. INTRODUCTION

The Z_2 oscillations in the electronic stopping cross sections superimposed on a smooth, monotonically-increasing function are a well-known phenomenon.[1-4] They arise from the nonmonotonous variations of the outer electron density for atoms of neighboring elements. These oscillations are most pronounced for low-energy heavy ions in the energy region below 1 MeV/amu, where most of the lost energy is transferred to the outer electrons of the target.

In the atomic units system ($m=e=\hbar=1$), which will be used throughout this work, the electronic stopping cross section can be written according to the Lindhard-Winther (LW) model[5] as

$$S_e=\frac{1}{N}\frac{dE}{dx}=\frac{4\pi[z_{1\ \mathrm{eff}}(v)]^2}{v^2}\int \rho(r)L(\rho(r),v)d^3r\,, \tag{1}$$

where $\rho(r)$ is the spatial charge distribution of the target electrons and $L(\rho,v)$ is the stopping function. The $Z_{1\ \mathrm{eff}}(v)$ is the projectile's effective charge and is almost independent of the Z_2 of the solid target.[6] In the high-energy region this expression converges to the Bethe-Bloch limit and becomes proportional to Z_2, independent of the exact shape of $\rho(r)$. On the other hand, at low projectile energies the main contribution to the integral comes from the outer electrons only. Knowledge of their density is therefore essential for the calculations of S_e. As the $\rho(r)$ function of the outer electrons is a nonmonotonous function of Z_2, oscillations in the stopping cross section will arise.

In our previous publication[7] a simple density model was introduced for the calculations of $\rho(r)$ in solids. It was based on the experimental volume-plasmon measurements and provided a good estimate of the real electronic charge distribution. This model and the method for the calculations of S_e will be briefly described in Sec. II. The results of the computations of S_e for H^+ and He^+ ions as a function of Z_2 and the basis of this model are presented in Sec. III and are compared with other calculations and experimental results.

In Sec. IV we discuss miscellaneous target effects. One important factor that has a bearing on the value of S_e is the solid target texture. As in the main only the density of the outer electrons is sensitive to the target-structure effects, this factor will influence mainly the low-energy projectile cross sections. A second effect commonly known in thin foils is the variation in the density of the target. This can be accounted for quantitatively within the framework of our model. Finally the relation between the solid-state information derived from Compton-profile experiments and low-energy electronic stopping cross sections is discussed.

II. DENSITY MODEL AND COMPUTATION METHOD

The electron density in solids can in principle be derived quite accurately from the free-atom (FA) wave functions, using the linear combination of atomic orbitals (LCAO) formalism. This formalism enables us to find the change in the wave function of an electron bound to a certain atom in the lattice, due to overlaps with wave functions of neighboring atomic electrons. In solids, and especially in metals, even overlaps of high-order neighbors are non-negligible for the outer weakly bound electrons. As a result the outer electrons are delocalized and an almost constant electron density is obtained in most of the atomic volume, while the core of inner-shell electrons is only

slightly affected by this interaction.

According to Eq. (1), S_e is computed from $\rho(r)$ through a functional relation using $L(\rho(r), v)$,[5] which is a moderate function of $\rho(r)$. The results are not very sensitive to the local details of $\rho(r)$. Therefore one can use an approximate electronic density, which resembles the main features of the LCAO density, but is much simpler to evaluate and yields correct results for S_e with relatively small effort.

This density model, which was developed in Ref. 7, assumes a constant electronic density C_0 in the outer region of the atom and a constant density correction C_i to the FA density in the inner region, such that the continuity of $\rho(r)$ on the boundary is satisfied. The constants, C_0, C_i, and the radius R, which defines the boundary between the outer and inner regions, are fixed by the following equations:

$$C_0(V_I - V_R) = N_{\text{eff}}\,, \tag{2}$$

$$\int_0^R 4\pi r^2 \rho_A(r)\,dr + C_i V_R = Z_2 - N_{\text{eff}}\,, \tag{3}$$

$$C_0 = C_i + \rho_A(R)\,, \tag{4}$$

where V_I is the atomic volume taken as 11.2 [atomic weight (g)]/[bulk density (g/cm^3)]; N_{eff} is the effective number of electrons participating in the volume-plasmon excitation,[8] as derived from experimentally-measured ω_p; $\rho_A(r)$ is the free-atom electron density[9]; and V_R ($=\frac{4}{3}\pi R^3$) is the volume of the inner atomic region. The input data are N_{eff}, V_I, and $\rho_A(r)$, while C_I, C_0, and R are derived from Eqs. (2)–(4).

As only a region with approximately constant electron density can sustain a well-defined plasma oscillation, N_{eff} represents those electrons which are spread in the outer region of the atom, a region with constant electron density. Equation (2) is based upon this assumption. Equation (3) results from Eq. (2) and from charge conservation in the atomic volume. Equation (4) expresses the continuity of $\rho(r)$ at $r=R$.

The electron density used in our approximation has the following form:

$$\begin{aligned} &\rho(r) = \rho_A(r) + C_i\,, \quad r < R\,, \\ &\rho(r) = C_0\,, \quad r \geq R\,. \end{aligned} \tag{5}$$

This electron-density function, when inserted into Eq. (1), yields the total electronic stopping cross section, comprised of two contributions, $S_p = S_{\text{in}} + S_{\text{out}}$, where

$$\begin{aligned} S_{\text{in}} &= \frac{4\pi}{v^2}\int_0^R \rho(r) L(\rho(r), v) 4\pi r^2\,dr\,, \\ S_{\text{out}} &= \frac{4\pi}{v^2}(V_I - V_R) C_0 L(C_0, v)\,. \end{aligned} \tag{6}$$

S_{in} and S_{out} are, respectively, are the inner and outer contributions of the electrons to the stopping cross section.

The calculations were done numerically. More details can be found in our previous paper.[1] The derived results for the electronic stopping cross sections of protons used $Z_{1\,\text{eff}}(v) = 1$, which is true for protons in solids at any velocity,[6] excluding only very low-electron-density metals. The computation of S_e for heavier projectiles requires a more accurate knowledge of $Z_{1\,\text{eff}}(v)$ than the present theories can provide. Fortunately $Z_{1\,\text{eff}}(v)$ in solid targets is almost independent of Z_2.[6] Therefore, if we define

$$Z_{1\,\text{eff}}(v) = \left(\frac{S_e(Z_1, Z_2, v)}{S_e(1, Z_2, v)}\right)^{1/2}$$

where $S_e(Z_1, Z_2, v)$ is the experimental electronic stopping cross section of the ion Z_1 in a target whose atomic number is Z_2, measured at a given

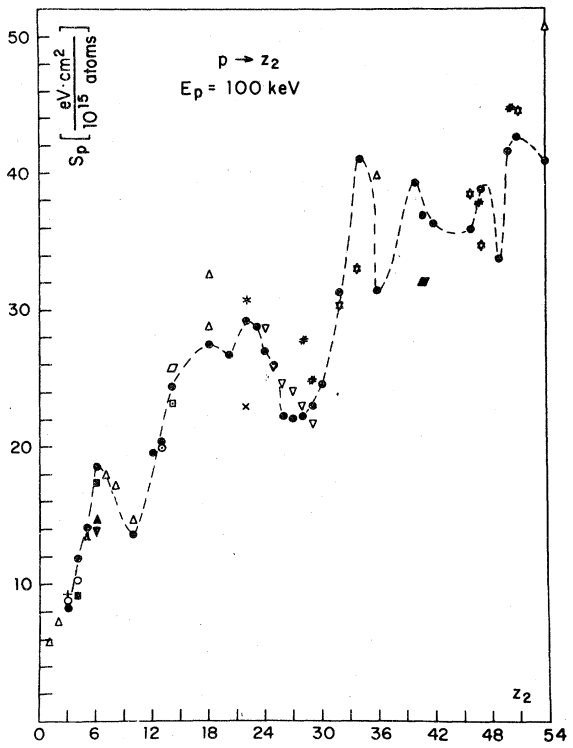

FIG. 1. Z_2 oscillations of S_e for protons at 100 keV. The closed circles are our computed values. The dashed line is drawn between them only to guide the eye. All the other points are experimental, with their references as indicated: △—Ref. 10, ○—Ref. 11, +—Ref. 12, ■—Ref. 13, ▲—Ref. 14, ▲—Ref. 15, ▼—Ref. 16, ⊠—Ref. 17, ⊙—Ref. 18, ⊡—Ref. 19, ▱—Ref. 20, *—Ref. 21, ×—Ref. 22, ▽—Ref. 23, #—Ref. 24, ▰—Ref. 25, ✡—Ref. 26.

velocity v; the resulting $Z_{1\,\mathrm{eff}}(v)$ will remain the same for any other target material at the same velocity v.

III. Z_2 OSCILLATIONS FOR H^+ AND He^+ IONS

As can be seen from Figs. 1–4, the agreement between the experimental Z_2 oscillations and our computational results is quite good in the amplitude as well as in the shape of the oscillations. We attribute this agreement to the fact that in our model the density of the outer electrons in the solids is derived from related experimental results. This is a simple procedure and still gives a good fit to the actual situation. The competing models use either the FA wave functions,[27] which give a rather poor approximation for the outer electron density in solids, or, when taking into account solid-state effects, complicated Korringa-Kohn-Rostoker band calculations[40] for deriving the electron density. The model of Latta and Scanlon[4] uses a modified electron density derived from the FA density with the aid of an arbitrarily defined free parameter.

Whereas for protons $Z_{1\,\mathrm{eff}}(v)=1$ can be safely used, for He ions $Z_{1\,\mathrm{eff}}(v)$ is energy dependent and reaches the value 2 only at relatively high energies. This fact was overlooked in some of the earlier computations.[27,40] We overcome this problem by using the experimental values of $Z_{1\,\mathrm{eff}}(v)$ for the ions, according to the procedure described in Sec. II. This is a better approach than that using the mean charge of the He ions emerging from solid targets, suggested in Ref. 4. The outgoing average charge may be determined by processes taking place after the emergence of the ion from the target, and therefore need not be the $Z_{1\,\mathrm{eff}}(v)$ of the projectile still traversing the solid foil.

When a comparison between the computed and the experimental values for the electronic stopping cross section is made, one has to be aware of the

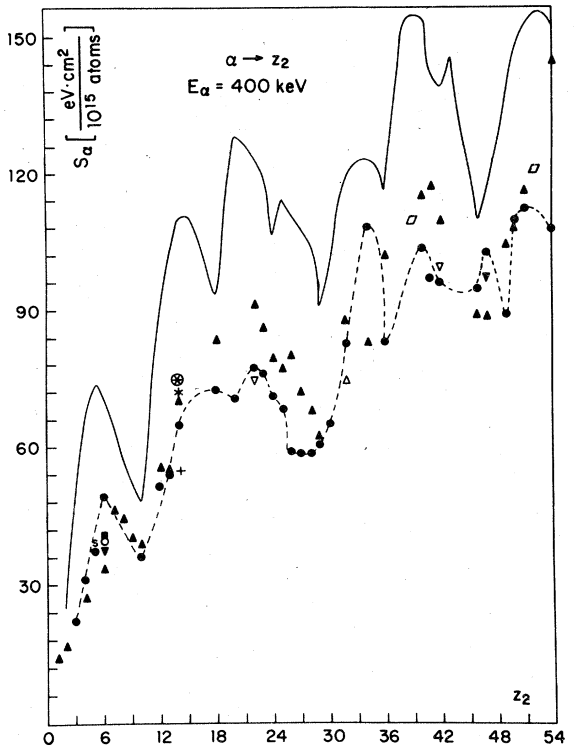

FIG. 2. Z_2 oscillations of S_e for α particles at 400 keV. The value of $Z^2_{1\,\mathrm{eff}}$ at this energy is, according to a large mass of experimental data, 2.64. The closed circles are our computed values. The dashed line is drawn between them only to guide the eye. The solid line is connecting the theoretically computed S_e values from Ref. 27. All the other points are experimental with their references as indicated: O—Ref. 7, ▲—Ref. 27, ▼—Ref. 28, ■—Ref. 29, + —Ref. 30, S—Ref. 31, *—Ref. 32, ⊛—Ref. 33, ▽—Ref. 34, △—Ref. 35, ▱—Ref. 36.

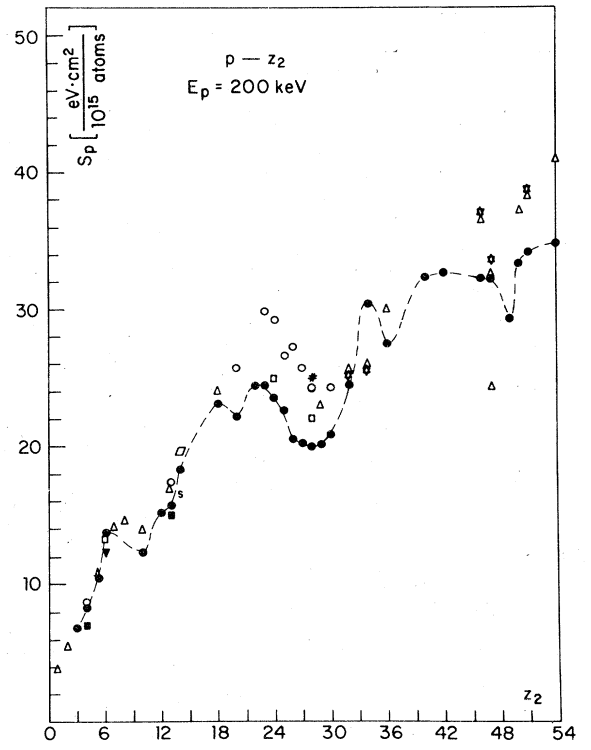

FIG. 3. Z_2 oscillations of S_e for protons at 200 keV. The closed circles are our computed values. The dashed line is drawn between them only to guide the eye. All the other points are experimental, with their references as indicated: □—Ref. 7, S—Ref. 37; for the other symbols see Fig. 1.

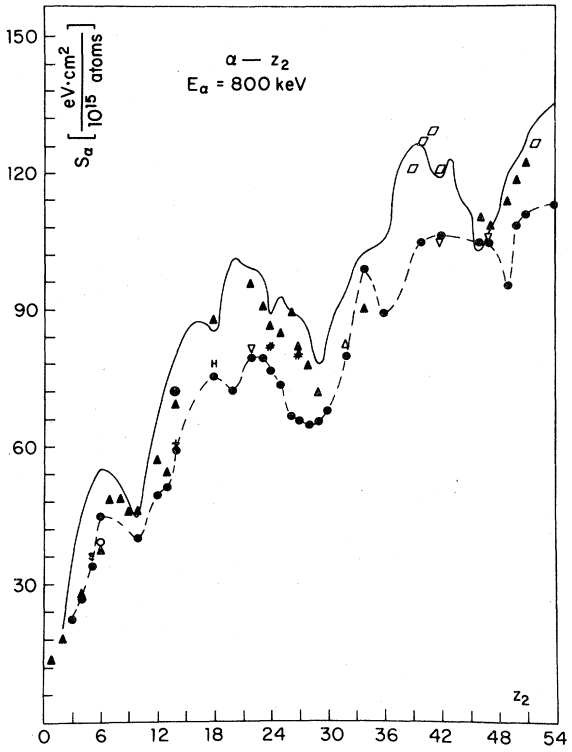

FIG. 4. Z_2 oscillations of S_e for α particles at 800 keV. The value of $Z_{1\,\mathrm{eff}}^2$ at this energy is, according to the existing experimental data, 3.25. The closed circles are our computed values; the dashed line is drawn between them only to guide the eye. The solid line is connecting the theoretically computed S_e values from Ref. 27. All the other points are experimental, with their references as indicated: S—Ref. 31, H—Ref. 38, #—Ref. 39; for the other symbols see Fig. 2.

fact that besides the well-known sources for the Z_2 oscillations, additional effects such as differences in target textures and densities should be considered. These effects, discussed in Secs. IV and V, may create additional maxima and minima in the experimental S_e curve, thus changing the oscillatory pattern in different sets of experiments. This can be seen for example by comparing the cross sections given in Figs. 1 and 2 in the Z_2= 22–29 region.

IV. TARGET-TEXTURE EFFECT

All the existing models for S_e calculations, including ours, take the relevant physical properties of the target, such as mean interatomic distance and atomic ordering from bulk data. However most of the S_e experiments, especially at low energies, are performed in thin foils. It is well known that the physical properties of thin foils may differ appreciably from those of bulk material.[29] Differences may occur also between thin foils of the same material, depending on the preparation conditions and the history of the foil.[41,42]

Such changes of physical properties are directly connected with changes of outer electron density, which in turn are the main contributors to the energy-loss-process of low-velocity ions. Differences between experimental S_e values in the same material are therefore expected. Examples can be seen in Fig. 1 for C, Si, Ti, and Ni and in Fig. 2 for C, Si, Ti, Ge, Mo, and Ag. Even larger differences may be found at still lower energies.

One possible change in the target properties, namely, the target density change, can be easily taken into account within the framework of our model, contrary to previous works, which discussed this effect only qualitatively.[29,32] One has only to vary V_I, which is inversely proportional to target density, and R, C_0, and C_i will be readjusted to satisfy Eqs. (2)–(4). The result of one such computation is shown in Fig. 5.

Another kind of target-structure effect is the long-range order. In materials possessing nonisotropic allotropic forms it may cause big changes in S_e, depending on the experimental setup. An example of anisotropic behavior of S_e, found by chance, is shown in Fig. 6. Here S_e for He^+ ions was measured with two kinds of evaporated carbon foils, manufactured by the Yissum Research Development Company. We measured the energy loss in targets set perpendicular to the beam direction and tilted at 60°. In one type of target called "strong" by the manufacturer the energy loss in the tilted target was doubled compared with the normal one, as expected from the $1/\cos\theta$ behavior of target thickness. Non-normal behavior was perceived in the second type of target, referred to as "superstrong." Although we were unable to get details of target preparation from the manufacturer, an electron microscopic analysis showed a high degree of single-crystal

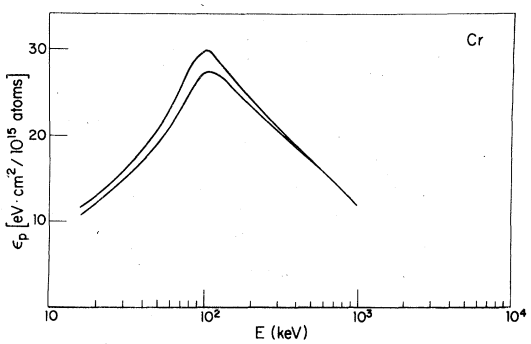

FIG. 5. Computed S_e results for Cr. The lower curve is calculated with the bulk density, while the upper one is computed assuming a 10% decrease in the foil density compared with bulk density.

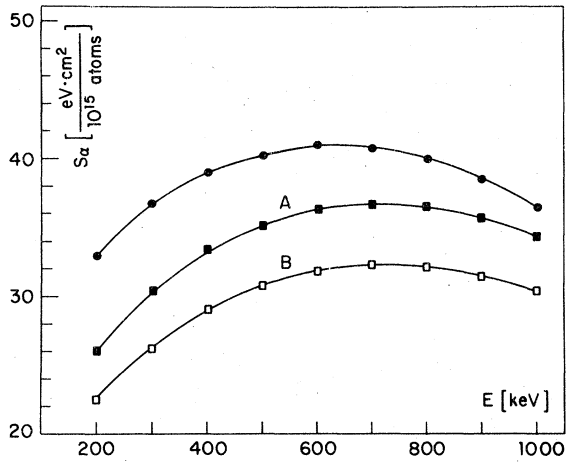

FIG. 6. Experimental S_e results for He^+ ions in two types of evaporated carbon foils. The circles refer to amorphous foil of the kind defined as "strong" in the text. The squares refer to foil mentioned as "superstrong" in the text. The curve labeled A is with the beam perpendicular to the foil, while the B curve is with target tilted at 60°, thus doubling its width.

structure in the superstrong sample, contrary to an almost perfectly amorphous structure in the strong foils. It is therefore recommended to verify the amorphous structure of the foils used as targets in S_e experiments simply by rotating them and checking whether the $1/\cos\theta$ behavior in the thickness is followed.

The Z_2 oscillations arising from electronic properties of the outer electrons can be seen also in Compton-profile measurements of the elements. An easy parameter to compare is $J(0) = 2\pi \int_0^\infty \langle \rho(\vec{P}) \rangle P\, dP$, where $\langle \rho(\vec{P}) \rangle$ is the spherical average of the Fourier transform of $\rho_0(r)$, the electron density. As the value of $J(0)$ is connected with the outer electron density, it displays Z_2 oscillations similar in shape, although not in amplitude, to those of S_e.[43]

Fortunately Compton-profile measurements performed in bulk do not suffer from the target-structure effects experienced in thin foils. They may therefore provide useful information as to which of the peaks and dips in the Z_2 oscillation curve are genuine and which are spurious, owing to target-structure effects. The shape of the oscillation in $J(0)$ for the $3d$ elements can be seen in Ref. 43. It agrees well with the shape of the oscillation in the stopping cross section as computed by us. We therefore believe that the small peak obtained for S_e in iron foils $Z_2 = 26$ as reported in Ref. 1 may be spurious, arising from target-structure effects.

Selenium constitutes a case in which the experimental values lie far below our calculated values. It is interesting to note that the Compton profile measurements yield a $J(0)$ value for selenium[44] much higher than that for its neighbor germanium. It is well known that selenium may occur in various allotropic forms, which may strongly affect the electronic stopping cross-section value.

V. CONCLUSIONS

The Z_2 oscillations in S_e are quite well reconstructed, using our simple density model. In thin foil targets, texture effects may cause fluctuations in S_e, depending on target-preparation technique and history. One cannot avoid the unfavorable conclusion that no model can fully account for the experimental values of S_e for heavy ions in the low-velocity region in thin foils. It is simply not a universal function. In this work we accounted for two additional factors in thin foils that affect S_e measurements, namely, density changes and long-range ordering. While a density change can be quantitatively treated within the framework of our model, a simple experimental test is recommended to avoid confusing results which may arise from accidental long-range ordering in the target.

This work has also pointed to the close linkage between Compton-scattering data and electronic-stopping cross section measurements. This connection may be used to deduce the real shape of Z_2 oscillations in S_e, free from other target-texture effects.

ACKNOWLEDGMENT

The authors would like to express their sincere thanks to Mr. J. Saban for his devoted technical assistance.

[1] W. K. Chu, D. Powers, Phys. Rev. 187, 478 (1969).
[2] C. C. Rosseau, W. K. Chu, and D. Powers, Phys. Rev. A 4, 1066 (1971).
[3] W. K. Chu and D. Powers, Phys. Lett. A 38, 267 (1972).
[4] B. M. Latta and P. J. Scanlon, Phys. Rev. A 12, 34 (1975).
[5] J. Lindhard and A. Winther, Dan. Widensk. Selsk. Mat. Fys. Medd 34, 4 (1964).
[6] W. Brandt, in *Atomic Collisions in Solids*, edited by S. Datz, B. R. Appleton, and C. D. Moak (Plenum, New York, 1975), Vol. I, p. 261.
[7] I. Gertner, M. Meron, and B. Rosner, Phys. Rev. A 18, 2022 (1978).
[8] D. Isaacson, New York University Radiation and Solid

State Lab. Internal Report, 1975 (unpublished).
[9]E. Clementi and C. Ruetti, At. Data Nucl. Data Tables 14, 177 (1974).
[10]S. K. Allison and S. D. Warshaw, Rev. Mod. Phys. 25, 779 (1953).
[11]M. Bader, R. E. Pixley, F. S. Mozer, and W. Whaling, Phys. Rev. 103, 32 (1956).
[12]W. D. Warters, W. A. Fowler, and C. C. Lavritsen, Phys. Rev. 91, 917 (1953).
[13]D. Kahn, Phys. Rev. 90, 506 (1953).
[14]J. C. Overly and W. Whaling, Phys. Rev. 128, 315 (1962).
[15]R. D. Moorhead, J. Appl. Phys. 36, 391 (1965).
[16]C. A. Sautter and E. J. Zimmerman, Phys. Rev. A 140, 490 (1965).
[17]A. Johansen, S. Steenstrup, and T. Wohlenberg, Radiat. Eff. 8, 31 (1971).
[18]W. White and R. M. Mueller, J. Appl. Phys. 38, 3660 (1967).
[19]C. Foster, W. H. Kool, W. F. Van der Weg, and H. E. Roosendaal, Radiat. Eff. 16, 139 (1972).
[20]A. Carnera, G. Della Mea, A. V. Drigo, S. LoRusso, and P. Mazzoldi, Phys. Rev. B 17, 3492 (1978).
[21]J. H. Ormrod, Nucl. Instrum. Methods 95, 49 (1971).
[22]E. M. Gunnersen and G. James, Nucl. Instrum. Methods 8, 173 (1960).
[23]W. White and R. M. Mueller, Phys. Rev. 187, 499 (1969).
[24]A. Valenzuela, W. Meckbach, A. J. Kestelman, and J. C. Eckardt, Phys. Rev. B 6, 95 (1972).
[25]R. Behrish and B. M. U. Schertzer, Thin Solid Films 19, 247 (1973).
[26]J. C. Eckardt, Phys. Rev. A 18, 426 (1978).
[27]J. F. Ziegler and W. K. Chu, At. Data Nucl. Data Tables 13, 479 (1974).
[28]D. I. Porat and K. Ramavataram, Proc. Phys. Soc. London 77, 97 (1961); 78, 1135 (1961).
[29]S. Matteson, E. K. L. Chau, and D. Powers, Phys. Rev. A 14, 169 (1976).
[30]D. Thompson and W. D. Mackintosh, J. Appl. Phys. 42, 3969 (1971).
[31]D. Kamke and P. Kramer, Z. Phys. 168, 465 (1962).
[32]J. F. Ziegler and M. H. Brodsky, J. Appl. Phys. 44, 188 (1973).
[33]F. H. Eisen, G. J. Clark, J. Bøttiger, and J. M. Poate, Radiat. Eff. 13, 93 (1972).
[34]E. Leminen and A. Fontell, Radiat. Eff. 22, 39 (1974).
[35]W. K. Lin, H. G. Olsen, and D. Powers, J. Appl. Phys. 44, 363 (1973).
[36]W. K. Lin, H. G. Olsen, and D. Powers, Phys. Rev. B 8, 1881 (1973).
[37]F. Cembali and F. Zignani, Radiat. Eff. 31, 169 (1977).
[38]U. Hoyer and H. Wäffler, Z. Naturforshg. A 26, 592 (1971).
[39]G. E. Hoffman and D. Powers, Phys. Rev. A 13, 2042 (1976).
[40]W. K. Chu, V. L. Moruzzi, and J. F. Ziegler, J. Appl. Phys. 46, 2817 (1975).
[41]H. H. Andersen, K. N. Tu, and J. F. Ziegler, Nucl. Instrum. Methods 149, 247 (1978).
[42]V. Sander and H. H. Bukow, Radiat. Eff. 40, 143 (1979).
[43]K.-F. Berggren, S. Manninen, T. Paakari, O. Aikala, and K. Mansikka, in *Compton Scattering*, edited by B. Williams (McGraw-Hill, New York, 1977), p. 160.
[44]U. Bonse, W. Schröder, and W. Schülke, Solid State Commun. B 21, 807 (1977).